FISEVIER

Contents lists available at ScienceDirect

Surface & Coatings Technology

journal homepage: www.elsevier.com/locate/surfcoat



Surface property modification of biocompatible material based on polylactic acid by ion implantation



I.A. Kurzina^{a,*}, O.A. Laput^a, D.A. Zuza^{a,b}, I.V. Vasenina^{a,c}, M.C. Salvadori^{a,d}, K.P. Savkin^b, D.N. Lytkina^a, V.V. Botvin^a, M.P. Kalashnikov^e

- ^a National Research Tomsk State University, 36 Lenin Ave, Tomsk 634050, Russia
- b Institute of High Current Electronics, 2/3 Akademicheskii Ave., Tomsk 634055, Russia
- ^c P.N. Lebedev Physical Institute, 53, Leninsky Prospect, Moscow, 119333, Russia
- d University of São Paulo, Matão Street, 1371-05508-090 São Paulo, SP, Brazil
- ^e National Research Tomsk Polytechnic University, 30 Lenin Ave, Tomsk 634050, Russia

ARTICLE INFO

Keywords: Biodegradable polymer Polylactic acid Ion implantation Degree of crystallinity Surface morphology Cytotoxicity

ABSTRACT

The investigations of the surface physicochemical and biological properties of polylactic acid modified by silver, argon and carbon ion implantation to doses of 1×10^{14} , 1×10^{15} and 1×10^{16} ion/cm² and energies of 20 keV (for C+ and Ar+) and 40 keV (for Ag²+) are described. X-ray photoelectron spectroscopy revealed that chemical bond ratio in polylactic acid is alternated indicating that different chemical processes take place depending on the implanted ion kind. Chemical reactions that occur during ion implantation of polylactic acid are proposed. X-ray diffraction analysis shows the degree of crystallinity decrease for all the ion types that leads to microhardness and elastic modulus decreasing. Silver is established to form metal nanoparticle into subsurface layer of polylactic acid with the average size of 2–3 nm. It was shown by atomic force microscopy that the higher irradiation doses the lower the surface roughness of polylactic acid that results in hydrophilicity improvement. The cytotoxicity investigation on three individual donor macrophages shows that Ag-implanted polylactic acid has no negative impact on the immune system cells and can be very promising material for biomedical application.

1. Introduction

Biodegradable materials based on polylactic acid (PLA) are widely used in biomedicine and tissue engineering because of their biocompatibility and their degradation to lactic acid in biological media [1]. These properties determine the interest in use of PLA for the production of biodegradable products with a short service life: self-absorbable surgical sutures, blood vessels, implants, biocompatible medical preparations, etc. [2,3]. Despite a number of advantages, polylactic acid has inert, hydrophobic surface due to the lack of specific functional groups, as well as low free surface energy, which prevents the attachment and proliferation of cells on surface [4]. This problem can be solved by surface modification of PLA with different nature ions [5,6].

Surface modification techniques allow changing of the physical and chemical properties of polymer materials with a wide range in the desired direction. Methods of surface irradiation with different charged particles are the most promising from the point of view of further application of the materials since at the variation of the conditions, the controlled surface property alteration occurs, without changing of the

bulk properties of the material [7]. Works on surface modification of polylactic acid and composite materials based on PLA by electron beams [8,9], using plasma flows [10,11], under the influence of laser [12] and

γ-irradiation [13] are of interest. Low-temperature plasma treatment is a perspective approach of surface modification of polylactic acid and materials based on PLA. The important point of plasma processing of PLA is the surface activation which is emergence of specific functional groups, increase in roughness, increase in free surface energy that leads to the material become more favorable for proliferation and cell growth [14]. It has been shown [15] that plasma treatment of polylactic acid surfaces causes roughness and increase in contact angle, and, in turn, increased roughness was found to improve PLA biocompatibility [16]. Moreover, the electron beam treatment of polylactic acid was established to result in a decrease in molecular weight by a factor of 3, which is associated with the processes of polymer chain scissions [17]. Changes in these properties can be essential for biomedical application of the polymer materials. By the way, other group revealed that electron-beam treatment of PLA results in degree of

E-mail address: kurzina99@mail.ru (I.A. Kurzina).

^{*} Corresponding author.

crystallinity increasing and development of the mechanical properties because of cross-linking and structural reorganization into the surface layer of the polymer [18]. In our previous papers [19,20] it was revealed that ion implantation and electron-beam treatment lead to wettability improvement and surface energy enhancement, as well as microhardness reduction and surface resistivity decrease.

Currently, the ion implantation of polymers is of a huge interest of many researchers. Ion implantation significantly affects on physical and chemical characteristics of the polylactic acid, at that the effects can be more dramatic than at the treatment of the material with electron beams and plasma flows. The possibility of different radiation processes initiation (degradation / cross-linking of the polymer chains at low dose implantation and carbonization of the polymer at the high dose implantation) during ion irradiation allows to control mechanical, optical and conductive properties of the polymer surface [21,22]. Polymer chain scission accompanied by surface oxidation processes and new functional group formation, which contribute to the material hydrophilicity, occurs as a consequence of ion implantation [23]. Ion implantation of carbon negative ions was found [24,6] to promote nervecell attachment and nerve line regeneration. It was found [25] the irradiation of gold and carbon negative ions allows controlling the surface morphology, e.g. roughness, which directly affects the attachment of neurons. Polylactic acid is widely used to build cell scaffolds for tissue engineering, hence surface morphology and its effect on biocompatibility of PLA is of great importance. Certainly, attaching the antibacterial properties to polymer materials is a current task, which can be solved by introducing silver ions into the surface layer of the material [26]. It was found that irradiation of PLA surface with inert gases ions (He, Kr, Ar) at energies up to 150 keV at doses of 1×10^{14} – 1×10^{15} ions/cm² results in cell adhesion improvement and a super-thin films, as well as self-assembled cell sheet formation [27]. This technique is promising for wound healing and the development of cellular technologies and clinical medicine.

The common problems and possibilities of changing the surface properties of materials based on polylactic acid are stated generally in the literature, while the most interesting questions are the chemical and physical processes occurring in the surface layers of the material under ion implantation. The effect of implantation of positively charged ions of silver, argon and carbon has not been completely investigated; chemical reactions occurring in the conditions of ion-beam treatment have not been proposed. Thus, this work is relevant today and is of scientific interest in the field of surface modification. The aim of the work described here was to study the influence of different ion nature implantation (metal – silver, inert gas – argon, nonmetal – carbon) at exposure doses of 1×10^{14} , 1×10^{15} , and 1×10^{16} ions/cm² on the surface physicochemical, functional and biological properties of PLA.

2. Materials and methods

2.1. Preparation of PLA samples

PLA samples were prepared by dissolving polylactic acid ([- OCH(CH $_3$)-CO-] $_n$) with molecular weight of 250,000 g/mol in chloroform at room temperature in a 7% solution [28]. The solvent was then removed by drying at room temperature in a Petri dish to form material with thickness $\sim\!\!1$ mm, then the PLA plates were cut into samples with area 10 \times 10 mm².

2.2. Ion implantation

Ion implantation was done using a facility incorporating our Mevva-V-Ru vacuum arc ion source [29]. This implantation facility operates in a repetitively pulsed mode with repetition rate 10 Hz and pulse duration 250 μ s. Ion kinds used in the present work were Ag, Ar and C. Charge state distributions of the ion beams were measured by a time-of-flight mass-to-charge spectrometer [30]. In this kind of ion source,

gaseous ions are singly ionized and hence we used Ar + ions. Metal ions are in general multiply ionized; for carbon the charge state of the extracted ion beam is singly ionized C⁺, while for silver the mean charge state of the extracted beam is 2+. Thus the implantation beams include Ag²⁺, Ar⁺ and C⁺ ions. Since the ion source extraction voltage was always 20 kV, the ion beam energies were 40 keV, 20 keV and 20 keV, respectively. For Ar⁺ ion generation we used the same ion source but somewhat modified to form a hollow cathode glow discharge mode [31]. Implantations were carried out to accumulated doses of 1×10^{14} , 1×10^{15} , and 1×10^{16} ions/cm². The implantation dose rate and average power density at the PLA target were adjusted by the ion beam current and pulse repetition rate, and were 1×10^{11} ions/(cm²·sec) and 0.5 mW/cm², respectively. The samples were mounted on a watercooled target holder whose temperature did not exceed 20 °C. A working pressure of 1×10^{-6} Torr was maintained by an oil-free highvacuum cryogenic pump.

2.3. Characterization techniques

The surface elemental composition was studied by X-ray photoemission spectroscopy (XPS) using K-Alpha+ Thermo Scientific Laboratory equipment with a $K_{\alpha}Al$ source. The samples were mounted on the standard $60\times60~\text{mm}^2$ K-Alpha top plate using conductive carbon tape or copper tape. The monochromated X-ray source was used for XPS analysis; this offers a user-selectable spot size from 30 to 400 μm , in steps of 5 μm . The 400 μm X-ray spot was used for high sensitivity and rapid analysis. The standard charge compensation system, employing very low energy electrons ($\sim\!0.1$ eV) and ions, was used during analysis. Cluster cleaning with the Monatomic and Gas Cluster Ion Source (MAGCIS) was performed on the samples. Phase composition was investigated by X-ray diffractometer XRD-7000S, Shimadzu with a $K_{\alpha}Cu$ source.

Surface morphology was studied by atomic force microscopy (AFM) using an NTEGRA Aura scanning probe microscope in tapping mode. The probe NSG01 of NT-MDT Spectrum Instruments with resonant frequency of 150 kHz, force constant of 5.1 N/m was employed, the scanning area was $50 \times 50 \, \mu m$; for the analysis the Gwyddion software was used. After survey the XY autoplane correction was performed. Transmission electron microscopy was carried out with a Jeol JEM-UC7. Samples were prepared using a Leica EM UC7 ultramicrotome, with a thin section of the starting material fixed to a 3 mm diameter mesh with an epoxy resin. Before placing the samples in the vacuum chamber of the microscope, a graphite current-conducting coating with a thickness of 1-2 nm was applied by magnetron sputtering. Water contact angles were measured by a sessile drop technique using a Kruss Easy Drop (DSA25) instrument. Mechanical properties of PLA (microhardness and elastic modulus) were measured with a Nanotest 600 hardness testing instrument using Berkovich tip at a load of 0.5 mN.

Cellular investigation was performed to primary evaluation of cytotoxicity. Human immune system cell (monocyte) reaction was investigated by cell-mediated immune response to monocytes CD14+. The monocytes from the blood of individual donors was separated [32], then cells was cultured in the presence of the samples for 6 days at 37 °C at the atmosphere of 7.5% $\rm CO_2$. Cells cultured without samples were used as control. The viability of cells was assessed after cultivation (evaluation of metabolic activity of cells). As a negative control (no living cells), a X-VIVO serum-free medium with the addition of Alamar Blue (volume of Alamar Blue/medium equal to 1/10) was used to measure the fluorescence signal, which was incubated for 3 h at 37 °C.

3. Results

3.1. Elemental and phase composition

The elemental and chemical composition of the polylactic acid samples implanted with silver, argon and carbon ions with an

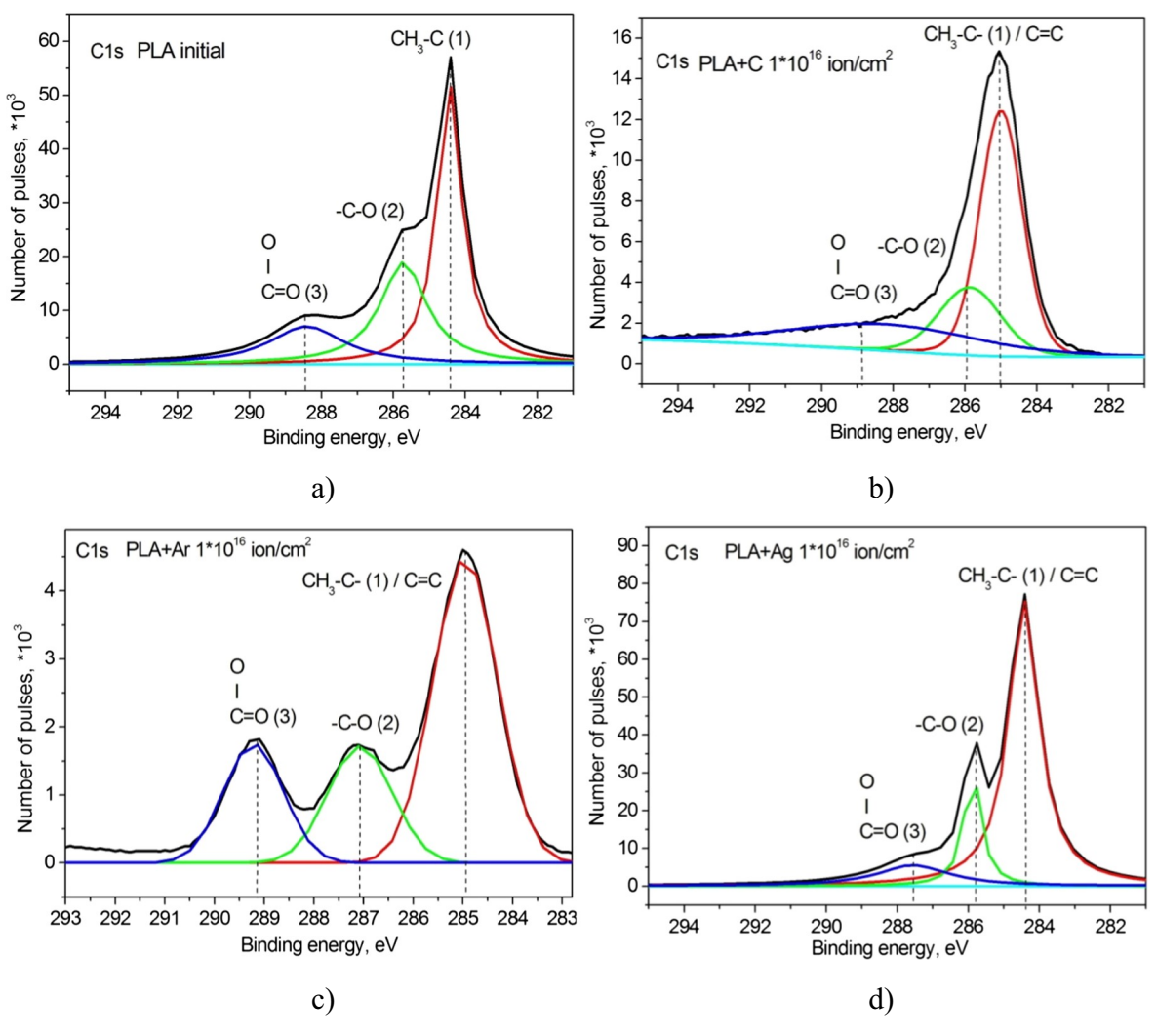


Fig. 1. XPS data C1s peak for initial and Ar-, Ag-, C-implanted PLA samples.

Table 1The position of C1s lines and the content of bonds in polylactic acid (The numbers in brackets correspond to the number of carbon and oxygen atoms in their various interactions according to the structural formula of the PLA).

+ÇH-Ç-Ö) n	Bond ratio in the C1s XPS spectrum, at. %		
¹CH₃ ¹O	CH ₃ -C (1)	-O-CH- (2)	O-C=O(3)
Sample	285.00	286.98	289.06
Binding energy, eV			
PLA initial	71	16	13
$PLA + Ag 1 \times 10^{16} ions/cm^2$	76	20	4
$PLA + Ar 1 \times 10^{16} ions/cm^2$	68	25	7
$PLA + C 1 \times 10^{16} ions/cm^2$	53	21	26

irradiation dose of 1×10^{16} ion / cm² was carried out by X-ray photoelectron spectroscopy and shown in the Fig. 1 [33,34]. According to the XPS data, it is established that the basic chemical composition of the surface of the PLA after implantation is preserved, no new bonds are formed. However, depending on the type of implanted ion, the bond ratio in C1s varies (Table 1). It was established that in the case of bombardment of Ag^{2^+} and Ar^+ there is a decrease in the contribution

of the O-C = O (3) bond and increase of peak area for -O-CH (2) bond in the C1s spectra of PLA. According to the presented lines in the XPS spectra, corresponding to the specific chemical bonds in the polymer, potential chemical reactions occurring in the surface layer during ion implantation can be proposed. It can be assumed that the decrease in the fraction of the carbonyl group O-C = O (3) up to 30% is due to the processes of decarbonylation and decarboxylation in macromolecules

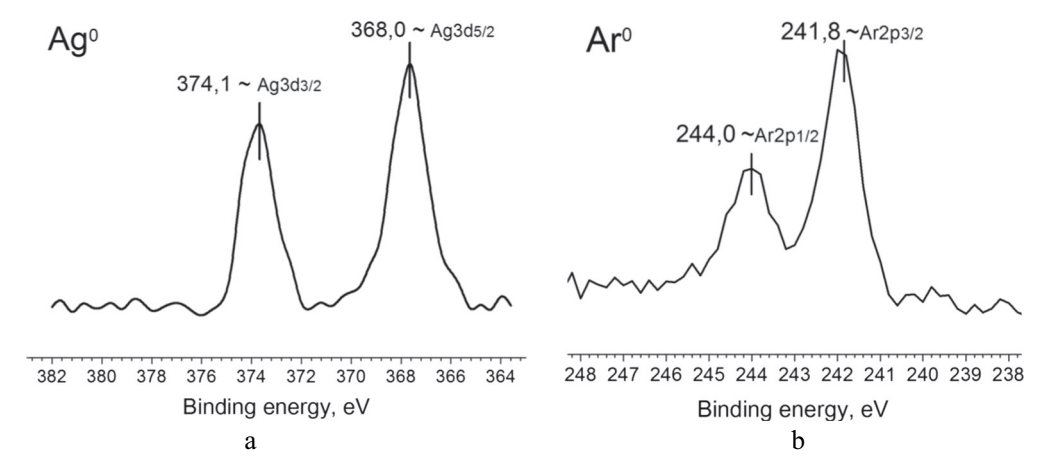


Fig. 2. XPS data Ag3d (a) and Ar2p (b) for Ag- and Ar-implanted PLA samples.

(Fig. 3, schemes 1,2). When implanted with Ar^+ and C^+ ions, the ratio of CH_3 -C (1) bond in the C1s spectrum is decreased due to polymer chain break and free radial formation. The appeared free radicals then can restore by cross-linking mechanism (Fig. 3, scheme 3). For C^+ -implanted PLA, the surface is oxidized accompanied by the C1s O-C=O (3) bond ratio increase twice. Alongside with that in case of Ar^+ implantation, the enhancement of -O-CH- (2) bond ratio in C1s of PLA is observed, which is associated with cross-linked macromolecule formation (Fig. 3, scheme 3).

Silver after ion implantation had been established to be in the metallic state, without forming a chemical bond with other atoms of the polymer (Fig. 2, a). The binding energy (E_b (Ag3d $_{5/2}$) = 368,0 eV, E_b (Ag3d $_{3/2}$) = 374,1 eV) of the silver atoms corresponds to the electrons at the 3d level of silver in zero oxidation state (metallic state of silver). The literature shows that metal nanoparticles may be formed under conditions of implantation of metal ions [35,36]. We assumed the formation of cation-pi interaction as a result of implantation of silver ions

in PLA and formation of silver nanoparticles in the polymer matrix (Fig. 3, scheme 4). For Ar⁺-implanted PLA sample, it was found low content of implanted argon atoms (\sim 0.6% by XPS). The Ar2p spectrum of argon contains two lines corresponding to the spin orbital components of Ar2p_{1/2} and Ar2p_{3/2} (Fig. 2,b). When C+ ions are implanted, the content of carbon are increased in the subsurface layer of PLA, but it is impossible to recognize the carbon of polymer chain and carbon that are embedded. In the ion implantation conditions, the C+ ions are restored to the atomic state and aggregated into clusters or particles (Fig. 3, scheme 5), as a result of which the atomic concentration of carbon increases. Moreover, in the process of ion implantation, polylactic acid undergoes radio thermolysis due to locally released energy in the ion track, which leads to a massive C-H break and some portion of C-C bonds (Fig. 3, schemes 1,2). The result is a gradual dehydrogenation of the polymer and the enrichment of its surface layer with carbon and oxygen (oxidation); excess carbon clusters to form polynuclear structures (Fig. 3, scheme 5).

Fig. 3. Proposed scheme of the processes taking place in the PLA under the conditions of ion-beam treatment.

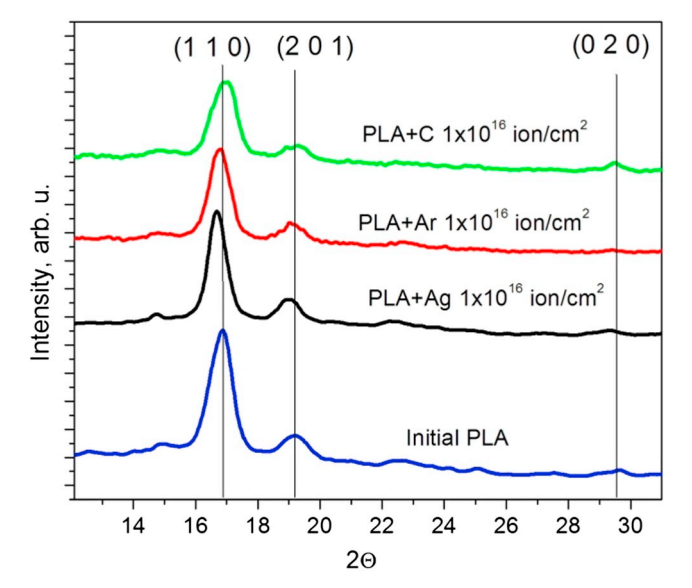


Fig. 4. Diffraction patterns of initial and Ag-, Ar-, C-implanted PLA samples.

Structure of polymers contains alternate ordered (crystal) amorphous areas. A degree of crystallinity of polylactic acid in the initial state depends on polymerization conditions. X-ray diffraction analysis revealed that there are two dominant peaks, typical for L-lactic acid isomer, correspondent to the angles $2\Theta \approx 19.1^{\circ} \text{ u } 16.9^{\circ}$ and crystallographic plane with the index (201), (110), respectively (Fig. 4). In addition, there is a low-grade peak $2\Theta \approx 29.5^{\circ}$, specific for (020) plane, in the initial and C-implanted samples, there is no such in other samples. The most stable form of poly-L-lactic acid is characterized by a orthorhombic crystal lattice with the following parameters: a = 10.66 Å, b = 6.16 Å, c = 28.88 Å [37]. The peak intensity decrease occurs depending on implanted ion species associated with PLA crystallographic parameter alteration (interplanar distance, coherentscattering region, degree of crystallinity; see Table 2) during implantation process. The degree of crystallinity is declined after ion implantation with the exposure dose increasing for all ion species, the maximum decrease is from 91% to 84% for 1×10^{16} ion/cm² C-implanted sample. Implantation of silver ions leads to an increase in the coherent scattering region up to 19 nm with an exposure dose increasing. In samples modified with carbon and argon ions, a decrease in crystallite size is observed, which does not change with an increase in the dose of implantation.

Changes in the structural-phase state of polymer in the ion implantation conditions are established to affect the surface mechanical properties. The microhardness and the elastic modulus of PLA decreases with the increasing of exposure dose and depend on the degree of crystallinity of the material (Table 2). Under the influence of ion

irradiation, an intensive thermal action takes place in the surface layer of a polymer, which leads to the restructuring of the material and reducing of areas with an ordered arrangement of PLA macromolecules, hence, the degree of crystallinity decreases.

3.2. Morphological characteristics

TEM images of PLA presented in Fig. 5 reveals that metal nanoparticles with average size of 2 nm and volume fraction of 15% are formed in the surface when PLA is implanted with Ag²⁺. On the other hand, areas with a lower packing density of macromolecules with the average size of 10 nm are observed when the samples are Ar- and Cimplanted as well as in the initial state of PLA. The pore formation in the initial material occurs when the solvent evaporates during the crystallization process. After implantation with carbon and argon ions, these pores are preserved; however, upon the implantation of silver ions, the pores merge ("fuse") and metal nanoparticles are formed. The absence of pores in the silver implanted PLA samples can be explained as follows. The average charge state of Ag ions in the experimental condition is 2+, but for Ar and C ions this is 1+. The energy of silver ions is higher and, therefore, the process of local heating of substrate while ion implantation is more intensively that leads to pore diminishing. Moreover, the radius of silver ions is greater than carbon and argon ion's one, which contributes to silver atom aggregation into the surface layer and metal nanoparticle formation.

In Fig. 6 the atomic force microscopy images of initial and 1×10^{16} ion/cm2 Ag-, Ar-, C-treated PLA samples are shown (adopted from [19]). The significant morphology modification was found to occur while ion implantation, which are dependent on the implanted ion kind. For all the implanted PLA samples, the roughness decreases with the exposure dose increasing (Table 3). For C-implanted PLA samples, the surface roughness is reduced from 167 nm for the dose of 1×10^{14} ions/cm² to 125 nm for the dose of 1×10^{16} ions/cm². When irradiated with argon ions, the roughness is reduced by 2.5 times in comparison with the initial sample (from 184 nm in the initial state to 76 nm for 1×10^{16} ions/cm² Ar-implanted PLA sample). Since the energy impact of silver ions during ion implantation is larger than for argon and carbon ion treatment (40 keV for Ag^{2+} and 20 keV for Ar^{+} and C^{+}), the initial large surface defects are crushed into the smaller ones when Ag ions are implanted. Therefore, the concentration of absorption centers is enhanced that leads to water contact angle decrease and, hence, the hydrophilicity increasing (Table 3). In addition to roughness, the contact angle can be affected by oxidation and carbonization processes during ion implantation. As it was shown earlier in this paper, ion-beam treatment of PLA results in oxygen-containing bonds increasing (Table 1) that promotes the hydrophilicity enhancement.

3.3. Biocompatibility of PLA

The primary evaluation of cytotocxicity with the macrophage of

Table 2Crystallographic parameters and mechanical properties of PLA before and after Ag, Ar, C ion-beam treatment.

Sample	Coherent-scattering region, nm	Degree of crystallinity, %	Microhardness, MPa	Elastic modulus, GPa
PLA initial	13	91	513,5	9,45
PLA + Ag 1 \times 10 ¹⁴ ions/cm ²	15	85	385,8	8,36
PLA + Ag 1 \times 10 ¹⁵ ions/cm ²	17	88	320,2	5,40
$PLA + Ag 1 \times 10^{16} ions/cm^2$	19	88	379,2	7,47
PLA + Ar 1 \times 10 ¹⁴ ions/cm ²	9	87	498,1	9,13
PLA + Ar 1 \times 10 ¹⁵ ions/cm ²	9	89	350,4	7,33
$PLA + Ar 1 \times 10^{16} ions/cm^2$	9	89	434,9	7,44
PLA + C 1 \times 10 ¹⁴ ions/cm ²	9	88	386,1	8,29
PLA + C 1 \times 10 ¹⁵ ions/cm ²	9	89	425,6	8,54
PLA + C 1 \times 10 ¹⁶ ions/cm ²	8	84	492,7	9,20

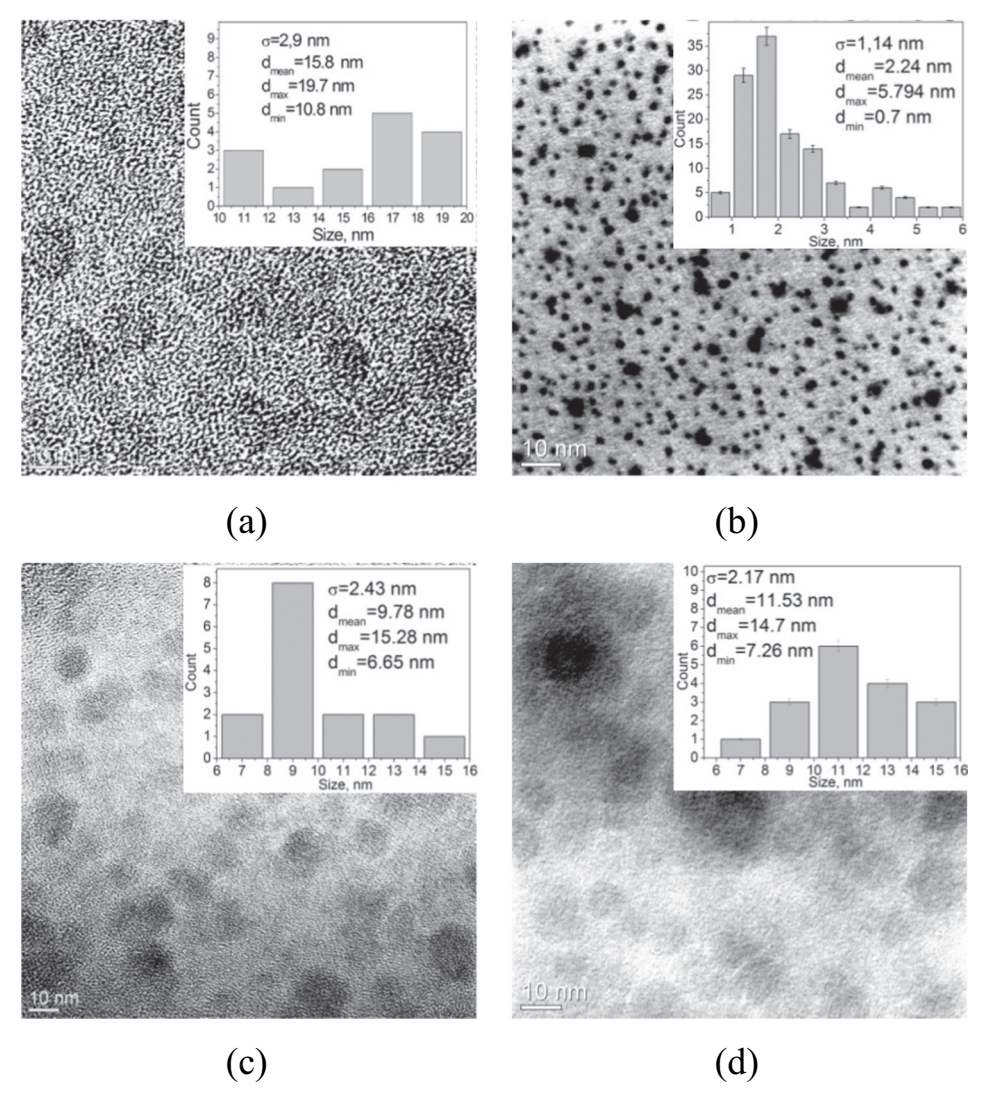


Fig. 5. TEM images of PLA samples: a) initial; b) Ag-; c) Ar-; d) C-implanted with the dose of 1×10^{16} ion/cm².

three individual donors reveals that both initial and 1×10^{15} , 1×10^{16} ion/cm² Ag-implanted PLA samples benefit the immune system cells (Fig. 7). The macrophage level after 6 days of culturing with PLA samples is comparable to the control sample (pure glass). It should be noted that when cells are interacted with Ag-implanted PLA sample, the cell survivability is decreased in relation to control and initial PLA sample, but the cells are rested alive. In addition, the viability of macrophages naturally is decreased with the exposure dose increasing, but in all samples (in the initial state and after ion implantation) it remains significantly higher than negative control, most cells remain viable. It was found that the amount of living immune system cells is slightly diminished in the presence of Ag on the PLA surface, however there is no sharp rejection of implanted material by biological medium.

4. Conclusion

The effect of 1×10^{14} , 1×10^{15} , 1×10^{16} ion/cm 2 Ag, Ar, C ion implantation on the PLA surface physicochemical, mechanical and biological properties was investigated. It was found that ion implantation influence on the elemental compound and structural-phase

composition. X-ray photoelectron spectroscopy revealed that chemical bond ratio in PLA is alternated indicating that different chemical processes (chain scission, free radical formation, gaseous product release, cross-linking, and carbonization) take place depending on the implanted ion kind. Chemical reactions that occur during ion implantation of PLA are proposed. The implanted silver does not form new chemical bonds with polymer molecules and aggregate metal nanoparticles with the average size of 2-3 nm into the PLA subsurface layer. XRD analysis revealed that coherent-scattering regions of PLA are enhanced due to ion bombardment and crystallographic parameter alteration. Moreover, the degree of crystallinity of PLA is decreased after surface modification that leads to mechanical properties (microhardness and elastic modulus) reducing. It was found out that the surface roughness increases when the exposure dose enhances, herewith the initial large defects are crushed into the smaller ones. The hydrophilicity enhancement is revealed to be dependent on the increase in the concentration of oxygen centers of adsorption and surface roughness. The primary evaluation of cytotocxicity with the macrophage of two individual donors was carried out and it was revealed that ion beam treated material does not negatively influence on immune system cells and can be promising for biomedical application.

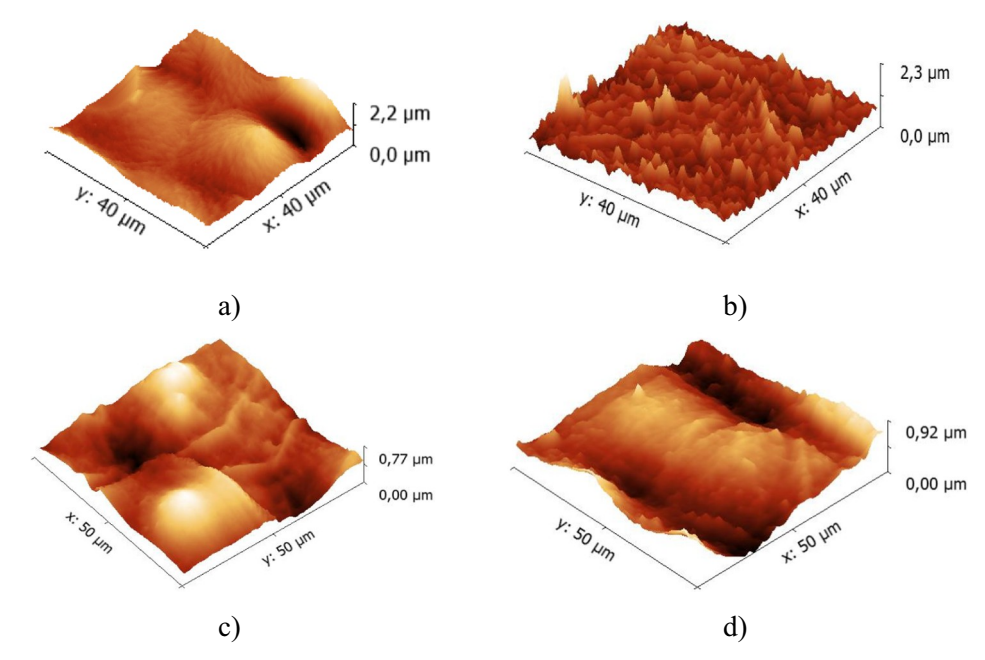


Fig. 6. AFM images of PLA samples: a) initial; b) Ag-; c) Ar-; d) C-implanted with the dose of 1×10^{16} ion/cm². (Adopted from [19])

 $\begin{tabular}{ll} \textbf{Table 3} \\ \textbf{Surface roughness and water contact angle of the initial and Ag-, Ar-, C-implanted PLA.} \\ \end{tabular}$

Sample	Roughness (R _a), nm	Water contact angle, °
PLA initial	184	77,1
PLA + Ag 1 \times 10 ¹⁴ ions/cm ²	138	70,4
PLA + Ag 1 \times 10 ¹⁵ ions/cm ²	104	65,6
PLA + Ag 1 \times 10 ¹⁶ ions/cm ²	88	62,2
PLA + Ar 1 \times 10 ¹⁴ ions/cm ²	127	68,6
PLA + Ar 1 \times 10 ¹⁵ ions/cm ²	96	65,2
PLA + Ar 1 \times 10 ¹⁶ ions/cm ²	76	64,0
PLA + C 1 \times 10 ¹⁴ ions/cm ²	167	75,1
PLA + C 1 \times 10 ¹⁵ ions/cm ²	138	71,1
PLA + C 1 \times 10 ¹⁶ ions/cm ²	125	67,1

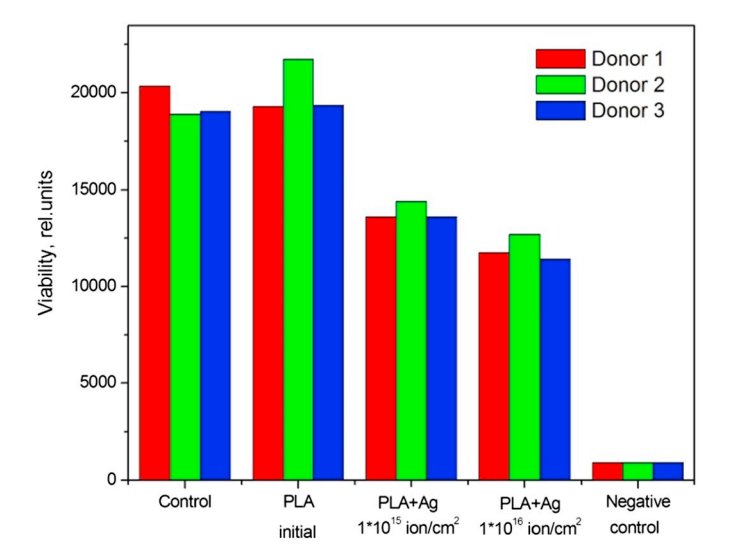


Fig. 7. Primary monocyte macrophages viability evaluation in vitro in the presence of PLA samples.

CRediT authorship contribution statement

I.A. Kurzina:Conceptualization, Methodology, Supervision.O.A. Laput:Investigation, Writing - original draft, Visualization.D.A. Zuza:Investigation, Writing - original draft, Visualization.I.V. Vasenina:Writing - review & editing, Validation, Visualization. M.C. Salvadori:Conceptualization, Methodology.K.P. Savkin: Conceptualization, Methodology.D.N. Lytkina:Conceptualization, Methodology.V.V. Botvin:Conceptualization, Methodology.M.P. Kalashnikov:Conceptualization, Methodology.

Declaration of competing interest

The authors declare that they have no known competing financial interests or personal relationships that could have appeared to influence the work reported in this paper.

Acknowledgments

This work was supported by the Tomsk State University competitiveness improvement program. Special thanks are extended to the Center for Collective Use of NR TSU, the Research Centre "Nanomaterials and Nanotechnologies" of NR TPU, the Laboratory of Thin Films of Institute of Physics of University of São Paulo and personally to A.V. Chernyavsky, K.V. Oskomov and V.V. Chebodaeva for assistance and support.

Appendix A. Supplementary data

Supplementary data to this article can be found online at https://doi.org/10.1016/j.surfcoat.2020.125529.

References

- [1] D.K. Gilding, A.M. Reed, Biodegradable polymers for use in surgery Polyglycolic-poly(acetic acid) homopolymers and copolymers: part 1, Polymer 20 (1979) 1459–1464, https://doi.org/10.1016/0032-3861(79)90009-0.
- [2] A.G. Miko, A.J. Thorsen, L.A. Czerwonka, Y. Bao, R. Langer, Preparation and characterization of poly(L-lactic acid) foams, Polymer 35 (1994) 1068–1077, https://doi.org/10.1016/0032-3861(94)90953-9.

- [3] C.M. Agrawal, R.B. Ray, Biodegradable polymeric scaffolds for musculoskeletal tissue engineering, J. Biomed. Mater. Res. 55 (2001) 141–150, https://doi.org/10. 1002/1097-4636(200105)55:2<141::AID-JBM1000>3.0.CO;2-J.
- [4] Z. Ma, C. Gao, J. Ji, J. Shen, Protein immobilization on the surface of poly-L-lactic acid films for improvement of cellular interactions, Eur. Polym. J. 38 (2002) 2279–2284, https://doi.org/10.1016/S0014-3057(02)00119-2.
- [5] T. Yotoriyama, A. Nakao, Y. Suzuki, T. Tsukamoto, M. Iwaki, Formation of a super-thin film and a self-assembly cellular sheet by ion-beam irradiation, Nucl. Inst. Methods Phys. Res. B 206 (2003) 527–531, https://doi.org/10.1016/S0168-583X (03)00778-X.
- [6] H. Tsuji, H. Sasaki, H. Sato, Y. Gotoh, J. Ishikawa, Neuron attachment properties of carbon negative-ion implanted bioabsorbable polymer of poly-lactic acid, Nucl. Inst. Methods Phys. Res. B 19 (2002) 815–819, https://doi.org/10.1016/S0168-583X(02)00659-6.
- [7] H.-J. Kwon, C.-H. Jung, D.-K. Kim, Y.-M. Lim, H.-K. Kim, Y.-C. Nho, J.-H. Choi, Biocompatibility improvement of polytetrauoroethylene by ion implantation, J. Korean Phys. Soc. 52 (3) (2008) 819–823, https://doi.org/10.3938/jkps.52.819.
- [8] H.-M. Ng, S.-T. Bee, C.T. Ratnam, L.T. Sin, Y.-Y. Phang, T.-T. Tee, A.R. Rahmat, Effectiveness of trimethylopropane trimethacrylate for the electron-beam-irradiation-induced cross-linking of polylactic acid, Nuclear Instruments and Methods in Physics B 319 (2014) 62–70, https://doi.org/10.1016/j.nimb.2013.10.027.
- [9] J.S.C. Loo, C.P. Ooi, F.Y.C. Boey, Degradation of poly (lactide-coglycolide) (PLGA) and poly(-lactide) (PLA) by electron beam radiation, Biomaterials 26 (2005) 1359–1367, https://doi.org/10.1016/j.biomaterials.2004.05.001.
- [10] J. Izdebska-Podsiadły, E. Dorsam, Effects of argon low temperature plasma on PLA film surface and aging behaviors, Vacuum 145 (2017) 278–284, https://doi.org/10. 1016/j.vacuum.2017.09.001.
- [11] P. Techaikool, D. Daranarong, J. Kongsuk, D. Boonyawan, N. Haron, W.S. Harley, K.A. Thomson, J. Foster, W. Punyodom, Effects of plasma treatment on biocompatibility of poly[(L-lactide)-co-(ε-caprolactone)] and poly[(L-lactide)-co-gly-colide] electrospun nanofibrous membranes, Society of Chemical Industry 66 (2017) 1640–1650, https://doi.org/10.1002/pi.5427.
- [12] K. Moraczewski, W. Mroz, B. Budner, R. Malinowski, M. Zenkiewicz, Laser modification of polylactide surface layer prior autocatalytic metallization, Surf. Coat. Technol. 304 (2016) 68–75, https://doi.org/10.1016/j.surfcoat.2016.06.085.
- [13] L. Zaidi, S. Bruzaud, M. Kaci, A. Boumaud, N. Gautier, Y. Grohens, The effects of gamma irradiation on the morphology and properties of polylactide/Cloisite 30B nanocomposites, Polym. Degrad. Stab. 98 (2013) 341–348, https://doi.org/10. 1016/j.polymdegradstab.2012.09.014.
- [14] M.-H. Ho, J.-J. Lee, S.-C. Fan, D.-M. Wang, L.-T. Hou, H.-J. Hsieh, J.-Y. Lai, Efficient modification on PLLA by ozone treatment for biomedical applications, Macromol. Biosci. 7 (2007) 467–474. https://doi.org/10.1002/mabi.200600241.
- [15] A.Y. Song, Y.A. Oh, S.H. Roh, J.H. Kim, S.C. Min, Cold oxygen plasma treatments for the improvement of the physicochemical and biodegradable properties of polylactic acid films for food packaging, J. Food Sci. 81 (1) (2016) 86–96, https://doi.org/10. 1111/1750-3841.13172.
- [16] S.I. Tverdokhlebov, E.N. Bolbasov, E.V. Shesterikov, L.V. Antonova, A.S. Golovkin, V.G. Matveeva, D.G. Petlin, Y.G. Anissimov, Modification of polylactic acid surface using RF plasma discharge with sputter deposition of a hydroxyapatite target for increased biocompatibility, Appl. Surf. Sci. 329 (2014) 1–18, https://doi.org/10.1016/j.apsusc.2014.12.127.
- [17] D.J. Leonard, L.T. Pick, D.F. Farrar, The modification of PLA and PLGA using Electron-beam radiation, J. Biomed. Mater. Res. A 89A (3) (2008) 567–574, https://doi.org/10.1002/jbm.a.31998.
- [18] S.T. Bee, C.T. Ratnam, T.S. Lee, T.T. Tee, W.-K. Wong, J.-X. Lee, A.R. Rahmat, Effects of electron beam irradiation on the structural properties of polylactic acid/ polyethylene blends, Nuclear Instruments and Methods in Physics Research 334 (2014) 18–27, https://doi.org/10.1016/j.nimb.2014.04.024.
- [19] I.V. Pukhova, K.P. Savkin, O.A. Laput, D.N. Lytkina, V.V. Botvin, A.V. Medovnik, I. A. Kurzina, Effect of ion-plasma and electron-beam treatment on surface

- physicochemical properties of polylactic acid, Applied Surface Science, 422 (2017) 856–862. doi:10.31554/978-5-7925-0524-7-2018-178-184.
- [20] I.V. Puhova, K.V. Rubtsov, I.A. Kurzina, A.V. Kazakov, A.V. Medovnik, Modification of polymer samples by electron beam treatment, Key Eng. Mater. 670 (2016) 118–125, https://doi.org/10.4028/www.scientific.net/KEM.670.118.
- [21] D.V. Sviridov, Ion implantation in polymers: chemical aspects, Chemical Problems of the Development of New Materials and Tehnologies 1 (2003) 88–106.
- [22] F. Sait, T. Yotoriyama, I. Nishiyama, Y. Suzuki, A. Goto, Y. Nagashima, T. Hyodo, Characterization of ion-irradiated poly-L-lactic acid using nano-cutting, Phys. Chem. Chem. Phys. 16 (2014) 26991–26996, https://doi.org/10.1039/ C4CD02763A
- [23] E. Sokullu-Urkac, A. Oztarhan, F. Tihminlioglu, A. Nikolaev, I. Brown, Oxidation behavior of metal ion implanted biodegradable polymers, IEEE Transactions on Plasma Science 40 (3) (2012) 863–869, https://doi.org/10.1109/TPS.2011. 2179677
- [24] J. Ishikawa, H. Tsuji, H. Sato, Y. Gotoh, Ion implantation of negative ions for cell growth manipulation and nervous system repair, Surf. Coat. Technol. 201 (2007) 8083–8090, https://doi.org/10.1016/j.surfcoat.2006.01.073.
- [25] E. Sokullu, F. Ersoy, A. Öztarhan, I.G. Brown, Controlling cell morphology on ion beam textured polymeric surfaces, Anatomy 9 (2015) 135–141, https://doi.org/10. 2399/ana.15.025.
- [26] E.E. Kocabas, O. Gube, E.M. Oks, G.Yu. Yushkov, A.G. Nikolaev, M.A. Oztarhan, Comparison of Antibacterial Properties of Ion Implanted and Conventional Nano Particle Treated Medical Textiles, 16th International Conference on Surface Modification of Materials by Ion Beams: Proceedings, PB-59, (2009).
- [27] T. Yotoriyama, A. Nakao, Y. Suzuki, T. Tsukamoto, M. Iwaki, Analysis of cell-adhesion surface induced by ion-beam irradiation into biodegradable polymer, Nucl. Inst. Methods Phys. Res. B 242 (2006) 51–54, https://doi.org/10.1016/j.nimb. 2005.08.201.
- [28] V.V. Botvin, E.G. Shapovalova, E.V. Zenkova, M.A. Pozdnyakov, Synthesis of glycolic and lactic acid oligomers, X International Conference of Students and Young Scientists "Prospects of Fundamental Sciences Development", (2013) 266–268.
- [29] A.G. Nikolaev, E.M. Oks, K.P. Savkin, G. Yu. Yushkov, I.G. Brown, Upgraded vacuum arc ion source for metal ion implantation, The Review of scientific instruments, 83, 2 (2012) 02A501. doi:https://doi.org/10.1063/1.3655529.
- [30] V.I. Gushenets, A.G. Nikolaev, E.M. Oks, L.G. Vintizenko, G. Yu, Yushkov, Simple and inexpensive time-of-flight charge-to-mass analyzer for ion beam source characterization // Review of scientific instruments 77 (2006) 063301, https://doi. org/10.1063/1.2206778.
- [31] G.Yu. Yushkov, R.A. MacGill, I.G. Brown, Mevva ion source operated in purely gaseous mode, Rev. Sci. Instrum. 75 (5) (2004) 1582–1584, https://doi.org/10. 1063/1.1691474.
- [32] A. Gratchev, M1 and M2 can be re-polarized by Th2 or Th1 cytokines respectively, and respond to exogenous danger signals, Immunobiology 211 (2006) 473–486, https://doi.org/10.1016/j.imbio.2006.05.017.
- [33] Z. Ding, J. Chen, S. Gao, J. Chang, J. Zhang, Immobilization of chitosan onto polyllactic acid film surface by plasma graft polymerization to control the morphology of fibroblast and liver cells, Biomaterials 25 (2004) 1059–1067, https://doi.org/10.1016/S0142-9612(03)00615-X.
- [34] J.-P. Chen, C.-H. Su, Surface modification of electrospun PLLA nanofibers by plasma treatment and cationized gelatin immobilization for cartilage tissue engineering, Acta Biomater. 7 (2011) 234–243, https://doi.org/10.1016/j.actbio.2010.08.015.
- [35] A.L. Stepanov, Optical properties of metal nanoparticles synthesized in the polymer by the method of ion implantation, J. Tech. Phys. 74 (2) (2004) 1–12 (in Russian).
- [36] V.N. Popok, Ion implantation of polymers: Formation of nanoparticulate materials Reviews on Advanced Materials Science 30 (2012) 1–26.
- [37] S. Sasaki, T. Asakura, Helix distortion and crystal structure of the α-form of poly (L-lactide), Macromolecules, 36 (2003) 8385–8390. doi:https://doi.org/10.1021/ ma0348674.